Research Article | DOI: 10.5281/zenodo.15712981
www.jnanosam.com

NANOSAM
Journal of NanoScience in Advanced Materials

Optoelectronic Characterization for Some of the Thermally Activated Delayed Fluorescence (TADF) Emitters Using Density Functional Theory (DFT)

Mona Sunaydih Alsaeedi[1,#]

Materials that exhibit thermally activated delayed fluorescence (TADF) are of great interest for organic light-emitting diodes (OLEDs) due to their ability to achieve 100% external quantum efficiency (EQE) without the need to incorporate heavy atoms. Since high-efficiency blue-emitting materials are still in demand, the pyrazine core was used in this study because of its high S_1 energy and weak electron-accepting ability. Therefore, pyrazine-based multi-carbazoles compounds 1–3 were studied using density functional theory (DFT) and time-dependent DFT (TD-DFT) methods. The simulated electronic and photophysical properties of the compounds agree with experimental observations. All compounds exhibit blue emission at 2.77, 2.68, and 2.62 eV, respectively. Replacing one biphenyl group with a carbazole unit (compound 2) decreases the E_{S1-T1} to 1.09 eV. Replacing two biphenyl groups with carbazole units (compound 3) further reduces E_{S1-T1} to 0.26 eV, facilitating the TADF mechanism. All compounds display mixed transitions of charge-transfer and locally excited character due to the increased donor ability with the addition of carbazole units.

1. Introduction

Thermally activated delayed fluorescence (TADF) compounds have been widely used in organic light-emitting diodes (OLEDs) as alternatives to noble metal complexes [1-3]. TADF compounds exhibit a unique endothermic photophysical process, called reverse intersystem crossing (RISC), which converts triplet excitons to singlet excitons (Figure 1) [4-6]. These compounds can achieve 100% internal quantum efficiency (IQE) when applied in OLEDs. For TADF to operate effectively, the energy gap between the S_1 and the T_1 states must be sufficiently small. This can be achieved by incorporating electron donor (D) and acceptor (A) moieties to adjust the highest occupied molecular orbitals (HOMO) and lowest unoccupied molecular orbitals (LUMO) at the donor and acceptor sites, respectively [4-6].

The small E_{S1-T1} is influenced by the nature of the S_1 states in TADF compounds. Mixed transitions involving charge transfer and locally excited character facilitate the ISC/RISC processes [7]. In this regard, multi-carbazole TADF materials have been widely investigated recently [6]. However, their intermolecular interactions in the triplet states led to form a persist dimerization, which in return lack the improvement of the photoluminescence quantum yields (PLYQs) and the colour stability in the OLEDs [6]. To enhance the electron-donating ability of the compounds with less capability of forming dimers, a weaker electron donor-acceptor systems like incorporated gradually instead of carbazoles. In addition to introducing a weak accepting unit of pyrazine to suppress the unpleasant interactions by arranging

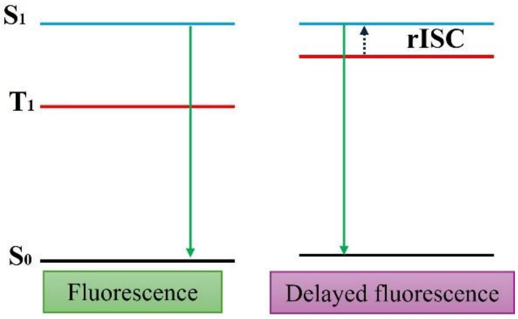

Figure 1. Schematic comparison between fluorescence and delayed fluorescence.

---

[1] *Department of Chemistry, College of Science, Taif University, Al-Haweiah, P.O. Box 11099, Taif 21944, Saudi Arabia.*

#Corresponding author: m.alsaeedi@tu.edu.sa

Keywords: Density Functional Theory (DFT); Thermally activated delayed fluorescence (TADF) emitters; Optoelectronic characterization

Received: 06 May 2025 | Accepted: 21 May 2025 | Published online: 26 June 2025

the carbazoles/biphenyls with minimum dihedral angles (Figure 2) [4,5].

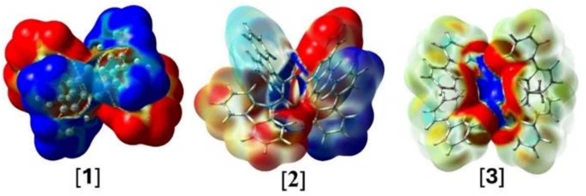

Figure 2. Electrostatic potential map [ESP] of compounds **1–3**.

In this study, a series of pyrazine-based multi-carbazole compounds synthesized by Eli Zysman-Colman et al. [4] and Saad Makhseed et al. [6] were theoretically designed and modeled (Figure 3). The electronic and photophysical properties of these compounds were examined using density functional theory (DFT) and time-dependent DFT (TD-DFT) methods.

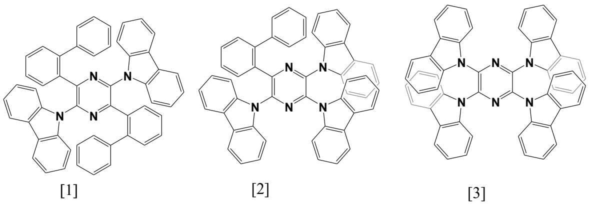

Figure 3. Structures of the thermally activated delayed fluorescence compounds **1–3**, under this study.

2. Computational details

Gaussian09 was used to optimize the ground and excited states of the compounds using DFT [8]. The restricted Becke, 3-parameter, Lee–Yang–Parr (B3LYP) model was used for ground-state optimization, while the unrestricted B3LYP method was applied to optimize the triplet states [9-11]. Vibrational frequencies were calculated to confirm that the optimized structures represent local minima. The compounds were optimized in toluene and acetonitrile using the polarizable continuum model, which accounts for electrostatic interactions with the solvent. Based on the optimized ground-state geometries, electronic transitions were calculated via TD-DFT, determining the energy and oscillator strength for the 25 lowest-energy singlet-singlet transitions. Additionally, the energies of the emissive states were obtained via TD-DFT by calculating the energy and oscillator strength for the 10 lowest-energy triplet molecular orbitals [9,12]. The calculated energy gaps and frontier molecular orbitals (FMOs) were visualized using Chemissian software.

3. Results and Discussion

The calculated energy diagram of the HOMO and LUMO levels of compounds **1–3** is shown in Fig.4, along with counterplots of the orbitals. The molecular orbital contributions are listed in Table S2 in the electronic supporting information (ESI).

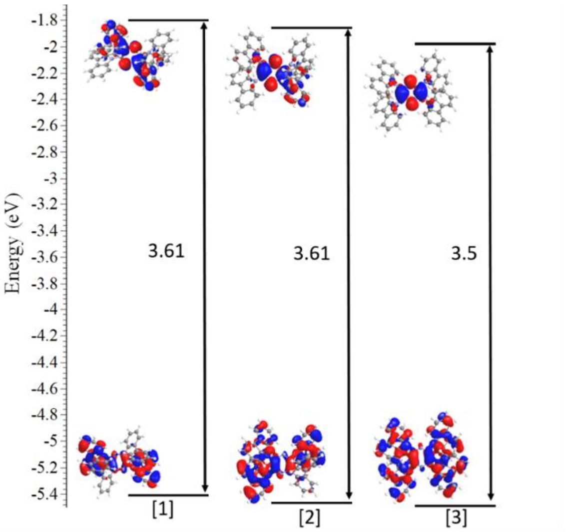

Figure 4. Calculated band gaps, HOMOs, and LUMOs of compounds **1–3** in toluene at B3LYP

Figure 4 shows that the HOMOs of compounds **1** and **2** are localized on the carbazole and pyrazine units, while their LUMOs are localized on the biphenyl and pyrazine units. In contrast, compound **3** shows the HOMO delocalized over the entire molecule, while the LUMO remains localized on the pyrazine. Increasing the electron-donating ability and the π-conjugation system (i.e., through the addition of carbazole units) stabilizes both the HOMOs and LUMOs of compounds **2** and **3**. The HOMO energy levels are -5.41, -5.46, and -5.48 eV, while the LUMO energy levels are -1.79, -1.85, and -1.97 eV for compounds **1–3**, respectively. All compounds show mixed transitions of charge transfer and locally excited character at longer wavelengths. The band gaps of compounds **1** and **2** are both 3.6 eV, while compound **3** exhibits a slightly narrower band gap of 3.5 eV, attributed to the greater π-conjugation from the additional carbazole units.

The singlet–singlet excitation energies for compounds **1–3** were determined using TD-DFT at the B3LYP level. The conductor-like polarizable continuum model was used to simulate the solvent effects of toluene and acetonitrile, as employed in the experimental setup. The absorption spectrum was simulated using Chemissian software with a half-bandwidth of 0.3 eV, along with the oscillator strengths (*f*) shown in Fig.5. The absorption wavelengths, oscillator strengths, dominant orbital excitations, and assignments of the singlet excited states are presented in Table 1. The lowest singlet–singlet absorption bands of compounds **1–3** were found at 413 nm (f = 0.07), 416 nm (f = 0.22), and 431 nm (f = 0.31), respectively. The red-shifted absorption of compound **3** at 431 nm is attributed to the stronger electron-donating effect and enhanced π-conjugation from the additional carbazole units. These theoretical results are in good agreement with the experimental absorption wavelengths of 388, 399, and 425 nm for compounds **1-3**, respectively.

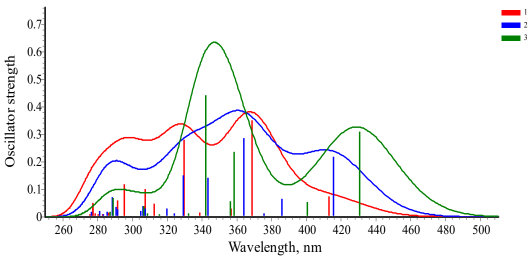

Figure 5. Simulated absorption spectra in toluene for [**1–3**], obtained at the B3LYP level.

Compounds **1–3** exhibited primarily HOMO → LUMO transitions, contributing approximately 70% to the $S_0 \rightarrow S_1$ transition. The compositions of the HOMOs in compounds **1–3** were 65% π and 35% n, while the LUMOs consisted of 67% π and 33% n for compound **1**, 57% π and 34% n for compound **2**, and 54% π and 46% n for compound **3**.

Compounds **1–3** displayed strong, intense absorption bands mainly attributed to π→π* transitions, located at 295 nm (f = 4.20), 288 nm (f = 4.29), and 289 nm (f = 4.29), respectively. These were assigned to HOMO–6 → LUMO transitions for compound **1**, HOMO–7 → LUMO transitions for compound **2**, and HOMO–1 → LUMO+3 transitions for compound **3**.

The low-lying singlet states of compounds **1–3** were calculated based on the optimized geometry of the first singlet excited state using the spin-restricted TD-DFT approach at the B3LYP level, showing good agreement with experimental data [4]. Based on the optimized S_1 structures, the emission energies, assignments, and transition characters of compounds **1–3** were calculated at the B3LYP level in toluene (Table 2) and in acetonitrile (Table S1).

Herein, the emission energies were determined using two different approaches (Figure 6). First, the adiabatic energy ($E_{0\text{-}0}$), representing the energy difference between the S_0 and the S_1 states in their respective optimized geometries, was calculated. This value reflects the nature of the emissive state and corresponds to the emission observed at 77 K [13]. This method was also used to calculate the energy difference between the T_1 and S_1 states ($E_{T1\text{-}S1}$), which helps estimate the potential for delayed fluorescence. Second, the vertical emission energy was calculated as the energy difference between the S_0 and the S_1 states, states based on the optimized geometry of the S_1 state [10,14].

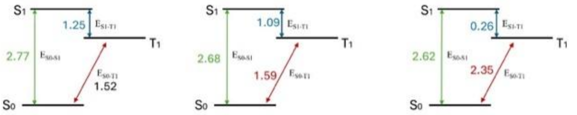

Figure 6. Schematic representation of Jablonski diagram for the TADF compounds **1–3**, calculated in toluene.

Overall, the lowest energy emissions calculated at the B3LYP level were in good agreement with experimental results, with a maximum deviation of 0.4 eV. The S_1 states were calculated to be at 2.77, 2.68, and 2.62 eV for compounds **1–3**, respectively, with corresponding $E_{T1\text{-}S1}$ values of 1.25, 1.09, and 0.26 eV. The broad, featureless emission bands indicate mixed LE and CT character. Notably, the adiabatic emission energies closely match those measured at 77 K, with a maximum deviation of 0.48 eV. Progressing from compound **1** to compound **3**, the emission energies and $E_{T1\text{-}S1}$ decrease, attributed to the increased electron-donating ability and π-conjugation (i.e., replacing biphenyls with carbazoles). These results are consistent with both experimental findings and previously published studies [4,6]. Furthermore, increasing the polarity of the solvent showed no significant influence on the emission energies (Table S3).

4. Conclusion

In this study, the electronic, absorption, and emission properties of a series of pyrazine-based multi-carbazole compounds were investigated using the TD-DFT method. The calculated absorption and emission features closely matched the reported experimental values. The results demonstrate that replacing biphenyl groups with carbazole units (compounds **2** and **3**) reduces the $E_{S1\text{-}T1}$ gap, facilitating the TADF mechanism. Further theoretical studies are needed to investigate the nature of the T_n states, as well as the transition dipole moments and dipole moment differences between the ground and excited states, to better estimate the likelihood of RISC occurring from T_n to S_1.

Table 1. Experimental and simulated electronic transitions of compounds **1-3** in toluene.

Compound	Absorption, λ_{max} (nm)	Molar Absorptivity ε ($\times 10^4$ M^{-1} cm^{-1})	Key Transitions (Major Contribution %)	Energy nm, (eV)	Oscillator Strength (a.u)	Nature
[1]	290 320 337 388	16.7 11.5 13.4 6.4	HOMO-6→LUMO (62) HOMO-4→LUMO (70) HOMO→LUMO+1 (70) HOMO→LUMO (70)	295, (4.20) 330, (3.76) 369, (3.36) 413, (3.00)	0.12 0.28 0.35 0.07	π→π* π→π* (CT+LE) (CT+LE)
[2]	288	26.3	HOMO-7→ LUMO (64) HOMO-10→ LUMO +1 (10)	288, (4.29)	0.07	π→π*
	320	13.4	HOMO→ LUMO +1(67) HOMO-2→ LUMO (11)	364, (3.40)	0.29	(CT+LE)
	332 399	15.8 10.9	HOMO→ LUMO (70)	416, (2.98)	0.22	(CT+LE)
[3]	320	265.5	HOMO -1→ LUMO +3 (61) HOMO -5→ LUMO +2 (19) HOMO -7→ LUMO +2 (13)	289, (4.29)	0.07	π→π*
	331	270.6	HOMO -1→ LUMO +1 (70)	342, (3.63)	0.44	(CT+LE)
	414 425	235.9 238.9	HOMO → LUMO (71)	431, (2.88)	0.31	(CT+LE)

[a] **H** and **L** denote HOMO and LUMO, respectively.

Table 2. Calculated lowest singlet excited states at the B3LYP level for compounds **1-3** in toluene, taking from the optimized structure of S_1

Compound	E_{RT}	E_{77K}	E_{S0-S1}	E_{S1-T1}	E_{S0-T1}	Key Transitions (Major Contributions %)	Energy (eV)	Oscillator Strength (a.u)	Nature
[1]	2.80	2.94	2.77	1.25	1.52	HOMO→ LUMO +1 (68) HOMO → LUMO (70)	370, (3.4) 380, (3.2)	0.39 0.03	(CT+LE)
[2]	2.70	3.06	2.68	1.09	1.59	HOMO → LUMO +1 +1 (68) HOMO -1→ LUMO +1 (71)	375, (3.3) 498, (2.5)	0.11 0.08	(CT+LE)
[3]	2.70	3.10	2.62	0.26	2.35	HOMO -1→ LUMO +1 +1 (70) HOMO → LUMO +1 (71)	342, (3.63) 431, (2,88)	0.45 0.31	(CT+LE)

Acknowledgements

I sincerely acknowledge the valuable contributions made by the following students: Amal Alharthi, Afnan Algoaid, Dhay Alotaibi, Hajar Alzharani, Nha Aladwani, and Rahaf AlRubaie.

Dedication

To real passionate students.

Authors' Contributions:

AK: Investigation, Resources, Data Curation, Formal analysis, Writing - Original Draft, Writing - Review & Editing.

Data Availability Statement

The data that support the findings of this study are available from the corresponding author upon reasonable request.

Declaration of Ethical Standards

The author(s) of this article declare that the materials and methods used in this study do not require ethical committee permission and/or legal-special permission.

Conflict of Interest

There is no conflict of interest in this study.

References

[1] Kessler, F., Watanabe. Y., Sasabe, H., Katagiri, H., Nazeeruddin, M.K., Grätzel, M., Kido, J., High-performance pure blue phosphorescent OLED using a novel bis-heteroleptic iridium(III) complex with fluorinated bipyridyl ligands. Journal of Materials Chemistry C. **1**(6), 1070–1075 (2013).

[2] Fan, C., Yang, C., Yellow/orange emissive heavy-metal complexes as phosphors in monochromatic and white organic light-emitting devices. Chemical Society Reviews. **43**(17), 6439–69 (2014).

[3] Pal, A.K., Krotkus, S., Fontani, M., Mackenzie, C.F., Cordes, D.B., Slawin, A.M., Samuel, I.D., Zysman-Colman, E., High-efficiency deep-blue-emitting organic light-emitting diodes based on iridium(III) carbene complexes. Advanced Materials. **30**(50), 1–10 (2018)

[4] Chen, D., Zhang, L., Matulaitis, T., Cordes, D.B., Slawin, A.M., Zhang, X.H., Samuel, I.D., Zysman-Colman, E., Tuning the emission and exciton utilization mechanisms of pyrazine-based multi-carbazole emitters and their use in organic light-emitting diodes. Journal of Materials Chemistry C. **11**(38), 13095–13105 (2023).

[5] Rajamalli, P., Chen, D., Suresh, S.M., Tsuchiya, Y., Adachi, C., Zysman-Colman, E., Planar and rigid pyrazine-based TADF emitter for deep blue bright organic light-emitting diodes. European Journal of Organic Chemistry. **2021**(16), 2285–2293 (2021).

[6] Salah, L., Etherington, M.K., Shuaib, A., Danos, A., Nazeer, A.A., Ghazal, B., Prlj, A., Turley, A.T., Mallick, A., McGonigal, P.R., Curchod, B.F., Suppressing dimer formation by increasing conformational freedom in multi-carbazole thermally activated delayed fluorescence emitters. Journal of Materials Chemistry C. **9**(1), 189–198 (2021).

[7] Wardle, B., *The physical deactivation of excited states*. (3) (Eds: Wardle, B), John Wiley & Sons (2009).

[8] Vlček, A., Záliš, S., Modeling of charge-transfer transitions and excited states in d6 transition metal complexes by DFT techniques. Coordination Chemistry Reviews. **251**(3–4), 258–287 (2007).

[9] Meng, X., Chen, M., Bai, R., He L., Cationic Iridium Complexes with 3,4,5-triphenyl-4H-1,2,4-triazole type cyclometalating ligands, synthesis, characterizations, and their use in light-emitting electrochemical cells. Inorganic Chemistry Journal. **59**(14), 9605–17 (2020).

[10] Costa, R.D., Ortí, E., Bolink, H.J., Graber, S., Schaffner, S., Neuburger, M., Housecroft, C.E., Constable, E.C., Archetype cationic iridium complexes and their use in solid-state light-emitting electrochemical cells. Advanced Functional Materials. **19**(21), 3456–3463 (2009).

[11] Costa, R.D., Ortí, E., Tordera, D., Pertegás, A., Bolink, H.J., Graber, S., Housecroft, C.E., Sachno, L., Neuburger, M., Constable, E.C., Stable and efficient solid-state light-emitting electrochemical cells based on a series of hydrophobic iridium complexes. Advanced Energy Materials. **1**(2), 282–290 (2011).

[12] Henwood, A.F., Pal, A.K., Cordes, D.B., Slawin, A.M., Rees, T.W., Momblona, C., Babaei, A., Pertegás, A., Orti, E., Bolink, H.J., Baranoff, E., Blue-emitting cationic iridium(III) complexes featuring pyridylpyrimidine ligands and their use in sky-blue electroluminescent devices. Journal of Materials Chemistry C. **5**(37), 9638–9650 (2017).

[13] Evariste S, Sandroni M, Rees TW, Roldán-Carmona C, Gil-Escrig L, Bolink HJ, et al. Fluorine-free blue-green emitters for light-emitting electrochemical cells. Journal of Materials Chemistry C.**2**(29), 5793–5804 (2014).

[14] Cortés-Arriagada D, Dreyse P, Salas F, González I. Insights into the luminescent properties of anionic cyclometalated iridium(III) complexes with ligands derived from natural products. International Journal of Quantum Chemistry. **118**(17), 1–12 (2018).